Anisotropic Phase Separation of a Nonequilibrium Liquid-Liquid Interface

C. K. Chan

Institute of Physics, Academia Sinica, Nankang, Taipei, Taiwan 11529, Republic of China

(Received 19 November 1993)

Dynamics of phase separations of a nonequilibrium diffuse transition interface with a thickness ζ of the order of 10 μm is studied in a binary liquid mixture by light scattering. We find that anisotropic growth in spinodal decomposition can be observed during the phase separations which form a sharp equilibrium interface, and that the dynamics can be scaled with ζ. Furthermore, a depletion layer is found to form around the sharp interface during the phase separation and gives rise to a diffractionlike light scattering pattern.

PACS numbers: 68.35.Rh, 05.70.Jk, 64.70.Ja

As phase separations in isotropic systems have been well studied, recent attentions have been turned to phase separations in systems with anisotropy such as phase separation of fluid mixtures under shear [1] and concentration gradients [2,3]. One naturally occurring anisotropy in liquid mixtures is the equilibrium transition interface separating the two coexisting concentrations at the final state of a phase separation. Although the equilibrium properties of such an interface have been studied [4], very little is known when the interface is out of equilibrium. For example, interesting phenomena might occur in the interface when the system is quenched deeper into the two phase region. Presumably, phase separation will be induced in both the interface and the bulk by such a quench, but it is not yet clear how phase separations in the interface will proceed [5,6].

In this Letter, we report the results of a light scattering experiment which studies the dynamics of phase separation of a transition interface similar to the one mentioned above in a binary liquid mixture. However, the interface under study is not in equilibrium with the bulk. This nonequilibrium interface is prepared by quenching an initially equilibrium interface at temperature T_i below T_c (critical temperature) to a temperature T_m above T_c. As mixing across the interface will occur at T_m, phase separations will take place in this nonequilibrium interface when the interface is quenched back to T_i again at a later time. Since the initial interface will be formed at the end of such a phase separation, our experiments essentially study how an equilibrium transition interface is formed from a phase separation under a spatially confined concentration gradient provided by the nonequilibrium interface. We find that anisotropic growth in spinodal decomposition (SD) can be observed in the phase separation and its dynamics scales with the thickness of the nonequilibrium interface, ζ. One striking feature of our findings is that a depletion layer is formed around the sharp interface during the phase separation and gives rise to a diffractionlike light scattering pattern [Fig. 2(b)].

A mixture of isobutyric acid and water (IBW) is used as our sample so that we can use pressure quenches to perform effective temperature quenches [7] and avoid convections caused by thermal quench [8]. The sample cell is a glass cylinder with an inner diametr of 2.8 cm and a length of 5.3 cm. While the top of the cell is sealed, a U-shaped capillary tube is attached to the bottom of the cell. A glass encapsulated magnetic stirrer is also kept inside the cell to provide means of mixing. The cell is first filled with a near critical sample of IBW (62.1 vol% water) [9] and then the capillary tube is filled with mercury to both seal the cell and provide a means of transmitting applied pressure. The sample is kept in a temperature-controlled, transparent water bath with a stability of ± 1 mK over a day. The critical temperature T_c of the sample is measured to be 26.9 °C with a drift of -0.3 mK per day because of the contact with mercury. Since we only perform pressure quenches, the bath is always kept at a constant temperature of $T = T_c - 40$ mK. All the temperature changes mentioned below are effective temperature changes produced by pressure changes. In order to study phase separation in the interface, a beam of a 5 mW He-Ne laser is directed through the interface (Fig. 1). Unless noted otherwise, the beam is always at an angle of $\theta = 6.75°$ with the tangent of the interface. A video system and a photodiode are placed outside the bath to record the small angle light scattering pattern on a screen and the reflected beam intensity, respectively.

Our experiment can be best understood by considering the time dependence of the reflected intensity of the laser beam $I(t)$ as shown in Fig. 1 for a typical experiment, with t being the time. Before the experiment starts ($t < A$), an equilibrium sharp interface was first prepared by placing an initially homogeneous sample at a temperature T_i below T_c for more than 48 h. The interface formed has a thickness with $\zeta \sim \xi$ (correlation length), and thus gives a reflected intensity I_0 which depends only on the reduced temperature $\varepsilon = (T_i - T_c)/T_c$. Therefore, the measured reduced reflectance $\rho(t) = I(t)/I_0$ is equal to 1 for $t < A$ as shown in Fig. 1. The experiment starts at $t = A$, when the sample is quenched to a mixing temperature T_m above T_c to let the two phases at either side of the originally sharp interface mix. Immediately after the sample is quenched into the one phase region, one can

0031-9007/94/72(18)/2915(4)$06.00

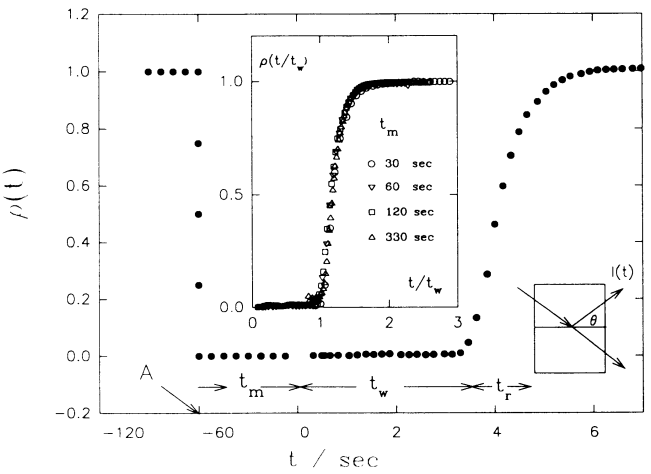

FIG. 1. The reduced reflectance $\rho(t)$ for an experiment of $T_i = T_c - 40$ mK and $T_m = T_c + 60$ mK and $t_m = 60$ sec. Note the change in the scale of time scale for $t < 0$. The left inset shows the scaling form of ρ for different t_m with t normalized by t_w. Geometry of the light scattering is shown in the right inset.

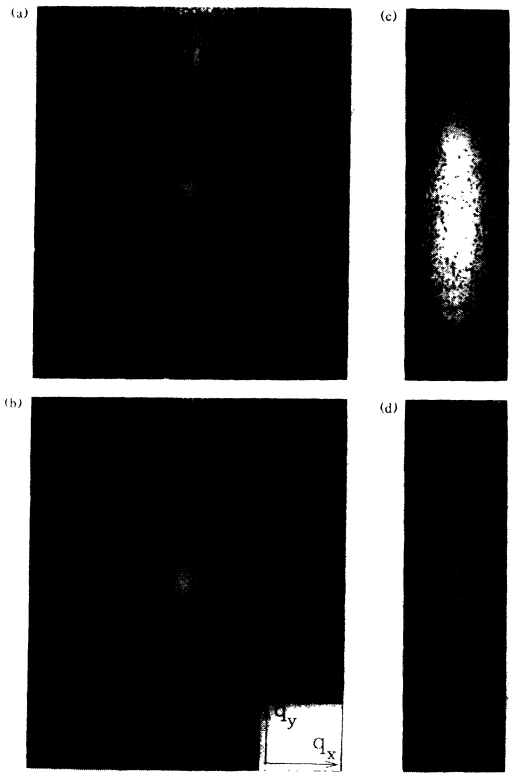

FIG. 2. Scattering patterns with different t_m for experiments of $T_i = T_c - 40$ mK and $T_m = T_c + 60$ mK. (a) $t = 2.5$ sec, (b) $t = 5$ sec for $t_m = 180$ sec, (c) $t = 25$ sec, and (d) $t = 35$ sec for $t_m = 480$ sec. Note that the central spot is the unscattered transmitted beam. Here q_x is in the horizontal direction.

see from Fig. 1 that the reflected beam disappears (point A in Fig. 1). Presumably, ζ has become much bigger than the wavelength of the laser beam in a very short time, and grows as $\zeta \sim (Dt)^{1/2}$ where D is the diffusion constant. The $(Dt)^{1/2}$ dependence of ζ is expected from the diffusion [10] across the initially sharp interface. Finally, in order to produce a phase separation in the interface, the sample is again quenched back to its initial temperature T_i after the sample is kept at T_m for a mixing time t_m at $t = 0$.

The $\rho(t)$ shown in Fig. 1 is taken from an experiment with $T_i = T_c - 40$ mK, $T_m = T_c + 60$ mK and a mixing time $t_m = 60$ sec. From Fig. 1, it can be seen that the reflected beam did not restore immediately after the temperature was quenched back to T_i. One has to wait for a while (t_w) in order to see the reflected beam again. Here t_w is defined as the time after the quench taken for the reflectance to recover 5% of its original value. But once the reflected beam becomes detectable, the measured reflectance quickly rises nearly to its original value before the quench. From Fig. 1, $\rho(t)$ rises nearly linearly from 10% to 80% in a recovery time t_r. Note that $t_w \sim 4t_r$.

The existence of two time scales t_w and t_r in Fig. 1 suggests that two different processes are responsible for the recovery of the interface. Presumably, t_w is the time taken for the phase separation in the diffuse interface to proceed to such an extent that a relatively sharp concentration profile is formed so that reflected light can be detected, and t_r is the time taken for this relatively sharp interface to recover the equilibrium sharp interface. Although only the data for $t_m = 60$ sec are shown in Fig. 1, the above observations are also true for experiments with different t_m. We find that both t_r and t_w vary as $t_m^{0.62}$ for fixed T_i and T_m. In fact, the measured $\rho(t)$ for various t_m can be put into a scaling form when the time is scaled by t_w, as shown in the inset of Fig. 1, which shows the scaled reduced reflectance for different t_m.

Now, we turn our attention to the forward scattering during the time $t > 0$ in Fig. 1. It is well known that small angle light scattering in the form of a collapsing ring can be observed during the SD of a critical binary mixture [10]. However, in our experiments, two rings, one fast and one slow, can be detected for experiments with $T_i = T_c - 40$ mK, $T_m = T_c + 60$ mK, and a mixing time t_m, of the order of minutes. A few tenths of a second after the sample is quenched back to T_i, a collapsing ring can be seen to emerge from the interface showing that phase separation is taking place. Several seconds after the first ring (fast) disappeared, a second ring (slow) emerges and collapses slowly in the order of minutes. Although the fast ring is similar to the spinodal ring in early time, it turns into an ellipse as shown in Fig. 2(a) with its minor axis parallel to the interface as it collapses. This suggests that the growth of the phase separating domains has become anisotropic. At an even later time, the ellipse will turn into two bright spots on either side of the central unscattered beam as shown in Fig. 2(b). These two bright spots last for only a few seconds,

and disappear when the slow ring becomes detectable. However, no anisotropy is detected in the slow ring within experimental precision.

For relatively short t_m, Figs. 2(a) and 2(b) describe well how the fast ring collapses. But for longer t_m, the scattering patterns change. Figures 2(c) and 2(d) show the scenario of the collapse of the fast ring with $t_m = 8$ min for the same experiment as in Figs. 2(a) and 2(b). With a longer mixing time, the fast ring does not collapse into two spots. Instead, the fast ring collapses to form a highly elongated, vertical, bright spot around the transmitted beam [Fig. 2(c)], showing that phase separating domains are large and elongated in the horizontal direction. However, as time goes on, this bright vertical spot will decrease in intensity and turn into a diffractionlike scattering pattern [Fig. 2(d)]. Similar to the two bright spots in Fig. 2(b), this scattering pattern disappears when the slow ring becomes visible.

To understand the above observations, we have shown in Fig. 3 the anticipated changes of concentration profile $C(z)$ during the experiment, where z is the distance from the position of $C(z) = C_c$, the critical concentration. Here, $C_0(z)$ of a sharp interface between two coexisting phases C_a and C_b in the beginning of the experiment at T_i is shown as circles. As the system is mixed for a time t_m at T_m, $C_0(z)$ will turn into $C'(z)$ with width $\zeta \sim (Dt_m)^{1/2}$, which is shown as triangles. When the system is quenched back to T_i, phase separation will take place at places where $C_a < C'(z) < C_b$. Since only a thin layer of fluid (SD layer) close to $z = 0$ with $C(z)$ close enough to C_c will undergo SD during phase separation [3], the rest of the fluid, region N in Fig. 3, will nucleate. Since SD is a much faster process than nucleation, a fast (SD) ring will be seen before the slow (nucleation) ring if we are probing the two regions of fluid at the same time as in our experiments.

Although it is not clear how $C'(z)$ will change in the SD layer during phase separations, a possible scenario is shown as the solid line in Fig. 3. Here the solid line depicts an instance that $C'(z)$ remains basically unchanged everywhere except in the SD layer, where it has already reached the equilibrium $C_0(z)$. This scenario is compatible with our observations that $\rho(t) = 1$ is recovered several seconds after the quench and the nucleation ring becomes observable only at a later time. Also, if one can approximate $C(z)$ by the form as shown in the left inset of Fig. 3, we will obtain a scattering pattern (right inset of Fig. 3) which is obtained from the FFT of the left inset. In fact, this scattering is compatible with our observation [Fig. 2(d)]. Note that the smooth rising part of the $C(z)$ is neglected in the calculation of the scattering pattern [11].

The sharp edges on either side of the interface (left inset) are important in producing the appropriate scattering pattern (right inset). If we have used a smooth decay on both sides of the interface, only the first peaks will be retained. This property of the sharpness of the edges is consistent with our observation in Fig. 2(b) that only two bright spots can be seen for short mixing time experiments. Presumably, for small ζ, effects of diffusion will smooth out the sharp edges. Note that the fluid immediately outside the two bumps is very similar to the depletion layer in nucleation theories [12], if we think of the bumps formed by SD as big droplets.

To understand the anisotropy in Fig. 2, we have plotted in Fig. 4 the time dependence of q_m in the vertical direction (q_{my}) and the horizontal direction (q_{mx}) for both the fast and slow rings. Here q_m is the magnitude of the scattering vector which corresponds to the maximum of the scattered intensity. If one looks at q_{mx}, its time dependence is very similar to that of normal spinodal decomposition [13] in the bulk, with $q_{mx} \sim t^{-a}$ and

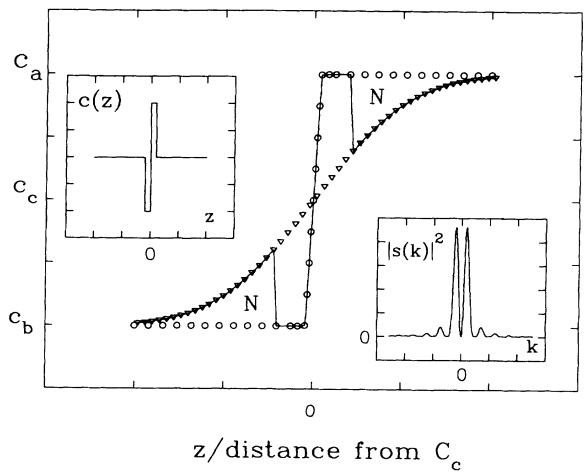

FIG. 3. Concentration profile across the interface at various times during phase separation. See text for detailed descriptions of symbols and insets.

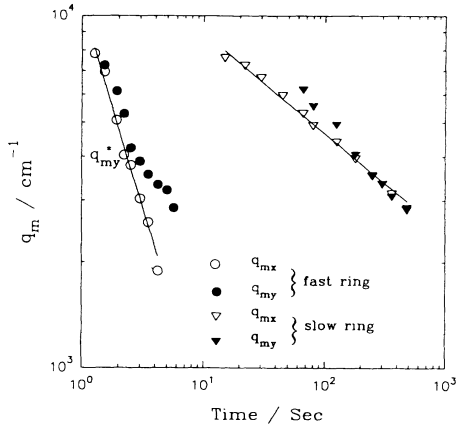

FIG. 4. The time dependence of the scattering vector q_m for both the fast ring and the slow ring in the vertical (q_{my}) and horizontal (q_{mx}) directions after a quench for an experiment of $T_i = T_c - 40$ mK, $T_m = T_c + 60$ mK, and a mixing time of 180 sec.

$a=-1.1$. However, the behavior of q_{my} is similar only for $q_{my} > q^*_{my}$ with $q^*_{my}=4\times10^3$ cm^{-1} as shown in Fig. 4. When $q_{my} < q^*_{my}$, the growth is slowed down and the scattering pattern will change from a ring into an ellipse [Fig. 1(b)]. Figure 4 also shows that for the slow ring, $q_{mx}=q_{my}\sim t^{-a}$, but with $a=0.31$, which is consistent with the notion that the slow ring is caused by nucleation [13]. The values of these exponents are consistent with a similar experiment reported by Beysens and co-workers [3]. With a very long mixing time (days) and different scattering geometry. However, no diffractionlike pattern and anisotropic growth in early time were reported in Ref. [3].

The meaning of q^*_{my} is clear when one considers the thickness of the diffuse interface. From $\zeta\sim(Dt_m)^{1/2}$, we obtain $\zeta\sim30$ μm for the experiment in Fig. 4. Growth has to be affected and stopped at around this length scale in the direction normal to the interface. In fact, ζ is of the same order of magnitude as the observed q^*_{my} in Fig. 4. To test the idea that the anisotropy is normal to the interface, we have also performed experiments with the laser beam perpendicular to the interface and find that two rings can be observed but without anisotropy. Furthermore, the waiting time t_w for the formation of a sharp interface can also be estimated by using ζ. Assuming that the phase separation in the interface is linear in time, as in the late time of SD [13], one then expects $t_w\sim\zeta\sim t_m^{-d}$ with $d=0.5$, which is not far from our measured value of 0.62.

From the above discussion, it seems that ζ is the length scale which determines the dynamics of the phase separation and the formation of a sharp interface. Although with ζ one can explain most of the observed phenomena quantitatively, it is still far from clear what kinds of processes are responsible for the formation of the final sharp interface. Presumably, peculiar structures of the anisotropic phase separating domains and hydrodynamics are responsible for the short time scale of t_r. Finally, it is important to note that our observed anisotropy is not due to the current driven by the concentration gradient which will produce anisotropy in a different direction as seen in driven diffusive systems [14].

The author would like to thank F. Perrot, W. I. Goldburg, Ki-Wing To, and A. Onuki for useful discussions. This work was conducted in the laboratory of W. I. Goldburg in Pittsburgh during a one year sabbatical leave of the author, supported by a grant from the NSC of Republic of China from 1992 to 1993.

[1] C. K. Chan, F. Perrot, and D. Beysens, Phys. Rev. Lett. **61**, 412 (1988).

[2] M. Kolb, T. Gobron, J.-F. Gouyet, and B. Sapoval, Europhys. Lett. **11**, 601 (1990).

[3] Y. Jayalakshmi, B. Khalil, and D. Beysens, Phys. Rev. Lett. **69**, 3088 (1992).

[4] J. W. Cahn and J. E. Hilliard, J. Chem. Phys. **28**, 258 (1958).

[5] D. Jasnow, D. A. Nicole, and T. Ohta, Phys. Rev. A **23**, 3192 (1981).

[6] S. N. Rauseo, N. Easwar, and J. V. Maher, Phys. Rev. A **35**, 3481 (1987).

[7] N.-C. Wong and C. M. Knobler, J. Chem. Phys. **66**, 4707 (1977).

[8] C. K. Chan, N. Y. Liang, and W. C. Liu, Rev. Sci. Instrum. **64**, 632 (1993).

[9] S. C. Greer, Phys. Rev. A **14**, 1770 (1976).

[10] H. S. Carslaw and J. C. Jaeger, *Conduction of Heat in Solids* (Oxford Univ. Press, New York, 1986), 2nd ed.

[11] The smooth part of $C(z)$ can be safely neglected, since no detectable scattering pattern can be observed immediately before the quench when only the smooth part of $C(z)$ is present.

[12] J. S. Langer, in *Fundamental Problems in Statistical Mechanics VI*, edited by E. G. D. Cohen (Elsevier Science Publishers B. V., Amsterdam, 1985).

[13] W. I. Goldburg, in *Light Scattering near Phase Transitions*, edited by H. Z. Cummins and A. P. Levanyuk (North-Holland, Amsterdam, 1983).

[14] C. Yeung, T. Rogers, A. Hernandez-Machado, and D. Jasnow, J. Stat. Phys. **66**, 1071 (1992).

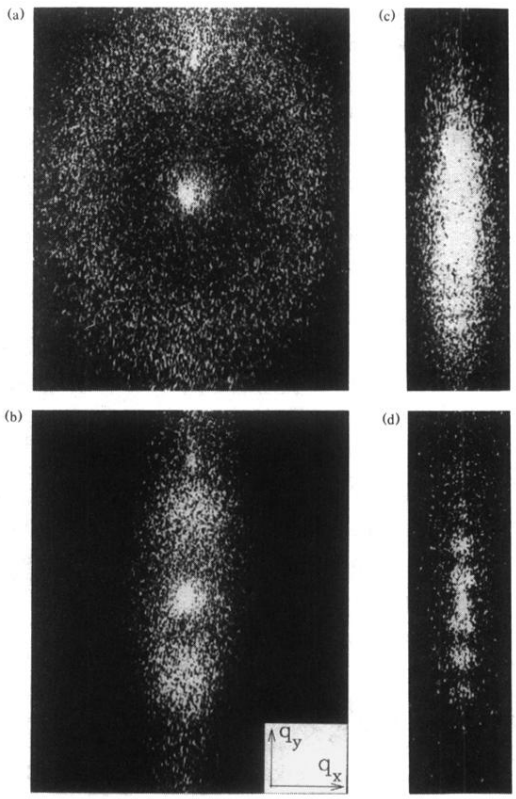

FIG. 2. Scattering patterns with different t_m for experiments of $T_i = T_c - 40$ mK and $T_m = T_c + 60$ mK. (a) $t = 2.5$ sec, (b) $t = 5$ sec for $t_m = 180$ sec, (c) $t = 25$ sec, and (d) $t = 35$ sec for $t_m = 480$ sec. Note that the central spot is the unscattered transmitted beam. Here q_x is in the horizontal direction.